Formal Mathematical Section: Orthospace Model for a Multi-FOV, Dual-Band Tumbler Afocal Module with Integrated Calibration

Notation and Preliminaries

We use bold lowercase for vectors (e.g., $\mathbf{x}$) and bold uppercase for matrices (e.g., $\mathbf{K}$). The unit sphere is $\mathbb{S}^2 \triangleq \{\hat{\mathbf{u}} \in \mathbb{R}^3 : \|\hat{\mathbf{u}}\|_2 = 1\}$. The special Euclidean group is $SE(3)$ and the special orthogonal group is $SO(3)$. For any nonzero $\mathbf{x} \in \mathbb{R}^n$, define

$$\mathrm{Norm}(\mathbf{x}) \triangleq \frac{\mathbf{x}}{\|\mathbf{x}\|_2}. \tag{1}$$

1 Coordinate Frames and State Space

Let $\mathcal{W}$ denote a fixed world coordinate frame and $\mathcal{C}$ denote the host camera reference frame rigidly attached to the detector focal plane array (FPA) and its native imager optical assembly.

The modular optical device defines a discrete set of electro-mechanically selectable configurations driven by a rotating tumbler. Let the tumbler assume one of N repeatable angular index positions:

$$\mathcal{I} \triangleq \{1, 2, \ldots, N\}. \tag{2}$$

Let $\mathcal{D}$ denote a device base frame fixed to the modular unit. Each index $i \in \mathcal{I}$ corresponds to a rigid transform from $\mathcal{D}$ into $\mathcal{C}$:

$${}^{\mathcal{C}}\mathbf{T}_{\mathcal{D}}(i) = \begin{bmatrix} {}^{\mathcal{C}}\mathbf{R}_{\mathcal{D}}(i) & {}^{\mathcal{C}}\mathbf{t}_{\mathcal{D}}(i) \\ \mathbf{0}^\top & 1 \end{bmatrix} \in SE(3), \tag{3}$$

where ${}^{\mathcal{C}}\mathbf{R}_{\mathcal{D}}(i) \in SO(3)$ and ${}^{\mathcal{C}}\mathbf{t}_{\mathcal{D}}(i) \in \mathbb{R}^3$.

Diagram: Frame Relationships and Discrete Tumbler States

2 Spectral Band Indexing and Observation Layers

Let $\mathcal{B}$ denote the set of spectral bands supported by the host dual-band camera system:

$$\mathcal{B} \triangleq \{b_1, b_2\}, \quad |\mathcal{B}| = 2. \tag{4}$$

Each $b \in \mathcal{B}$ induces band-specific intrinsics, distortion, and radiometric response parameters.

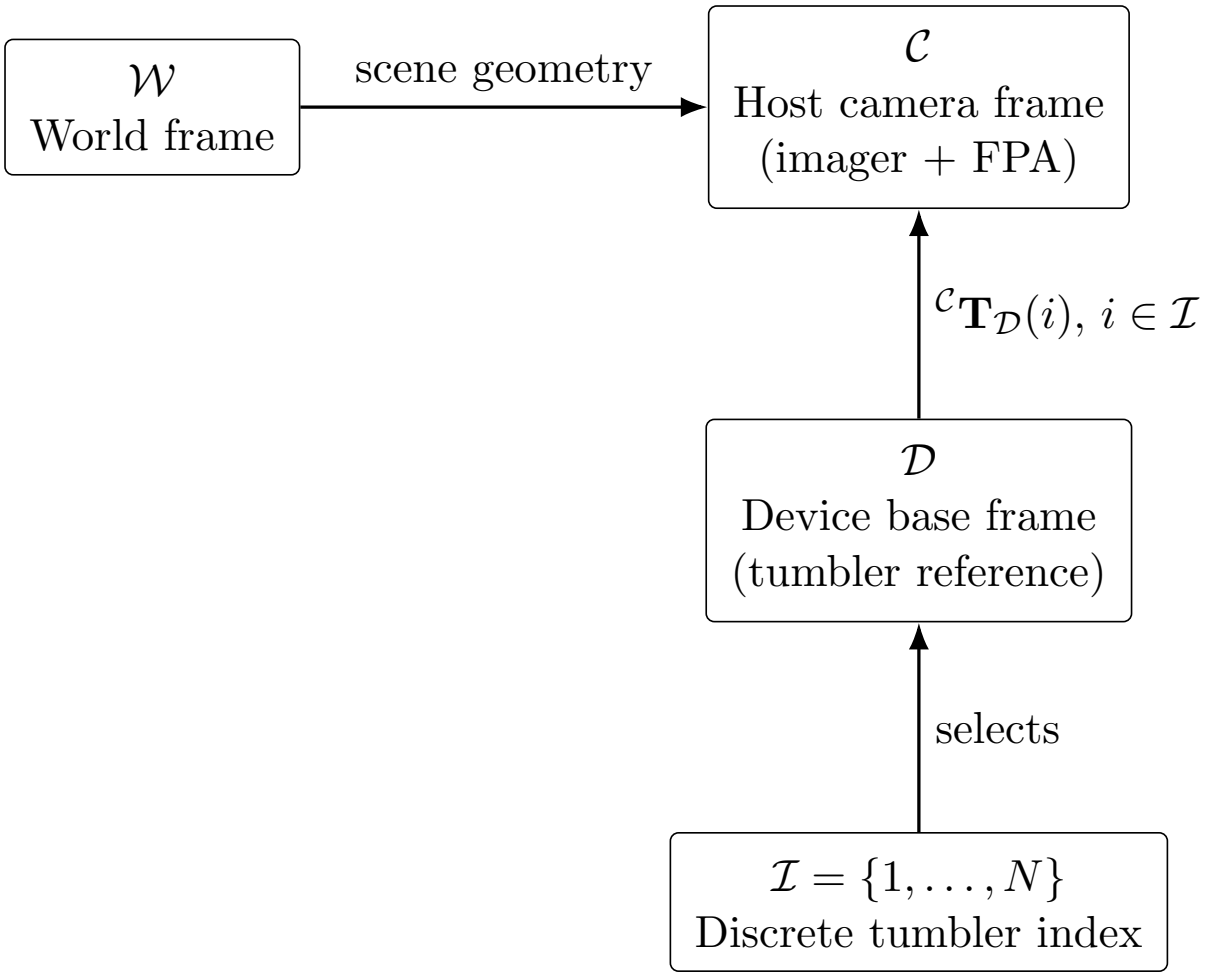

Figure 1: Coordinate frames and the discrete configuration index induced by the electromechanical tumbler.

3 Afocal Galilean Assemblies as Direction-Space Operators

A Galilean afocal telescope maps input ray direction to output ray direction without forming an intermediate image plane. Accordingly, the natural mathematical object is a mapping on the unit sphere of directions.

Let an incident ray in camera coordinates be represented by a unit direction vector:

$$\hat{\mathbf{u}} \in \mathbb{S}^2 \subset \mathbb{R}^3. \tag{5}$$

For each selectable optical path p and spectral band b, define the direction-space mapping:

$$\hat{\mathbf{u}}' = \Phi_{p,b}\big(\hat{\mathbf{u}}\big), \qquad \Phi_{p,b} : \mathbb{S}^2 \to \mathbb{S}^2. \tag{6}$$

A first-order afocal model may be represented as an angular scaling about an optical axis $\hat{\mathbf{a}}_p(i)$ (dependent on tumbler state i), with magnification $M_{p,b}$ (Galilean angular magnification; typically $|M_{p,b}| > 1$ narrows the FOV):

$$\Phi_{p,b}(\hat{\mathbf{u}}) \approx \mathrm{Norm}\left(\hat{\mathbf{a}}_p(i) + \frac{1}{M_{p,b}}\left(\hat{\mathbf{u}} - (\hat{\mathbf{u}} \cdot \hat{\mathbf{a}}_p(i))\hat{\mathbf{a}}_p(i)\right)\right). \tag{7}$$

More generally, $\Phi_{p,b}$ may be implemented as a calibrated function (e.g., polynomial, spline, or ray-trace derived LUT) to absorb higher-order distortion:

$$\Phi_{p,b}(\hat{\mathbf{u}}) \triangleq \mathrm{LUT}_{p,b}(\hat{\mathbf{u}}). \tag{8}$$

Diagram: Direction-Space Mapping and Host Projection

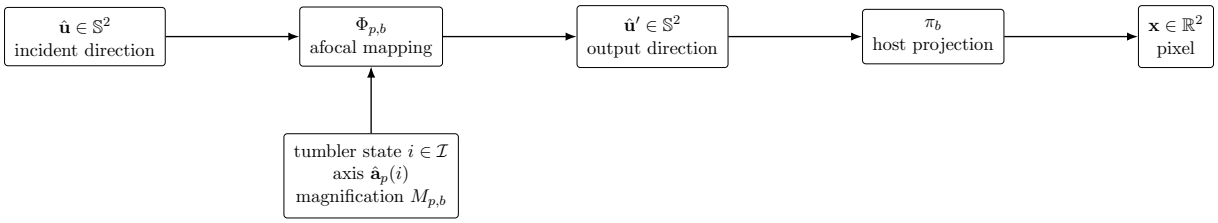

Figure 2: Afocal direction-space mapping composed with the host camera projection per band.

4 Orthogonality Constraint Between Afocal Assemblies

The modular device houses two orthogonal Galilean afocal optical assemblies. Let the optical axes for these assemblies, in the device frame $\mathcal{D}$, be $\hat{\mathbf{a}}_1^{\mathcal{D}}$ and $\hat{\mathbf{a}}_2^{\mathcal{D}}$. Orthogonality is expressed as:

$$\hat{\mathbf{a}}_1^{\mathcal{D}} \cdot \hat{\mathbf{a}}_2^{\mathcal{D}} = 0. \tag{9}$$

Under tumbler index i, the axes expressed in the camera frame are:

$$\hat{\mathbf{a}}_m(i) = {}^{\mathcal{C}}\mathbf{R}_{\mathcal{D}}(i)\, \hat{\mathbf{a}}_m^{\mathcal{D}}, \quad m \in \{1, 2\}. \tag{10}$$

Orthogonality is preserved:

$$\hat{\mathbf{a}}_1(i) \cdot \hat{\mathbf{a}}_2(i) = 0, \ \ \forall i \in \mathcal{I}. \tag{11}$$

This orthogonality is the core "Orthospace" property: the device provides multiple fields of view corresponding to projections along mutually orthogonal basis directions, enabling structured multi-projection sensing.

Diagram: Orthogonal Afocal Axes in the Camera Frame

5 Host Imager Projection Model

Let the host camera's imager optical assembly and FPA define an image formation model per band:

$$\pi_b : \mathbb{S}^2 \to \mathbb{R}^2. \tag{12}$$

A standard central projection with distortion can be written as:

$$\mathbf{x} = \pi_b(\hat{\mathbf{u}}') = \mathbf{K}_b \begin{bmatrix} u'_x/u'_z \\ u'_y/u'_z \\ 1 \end{bmatrix} + \mathbf{d}_b(\hat{\mathbf{u}}'). \tag{13}$$

The modular device composes with the host model by modifying the effective incident direction via $\Phi_{p,b}$ and the tumbler state.

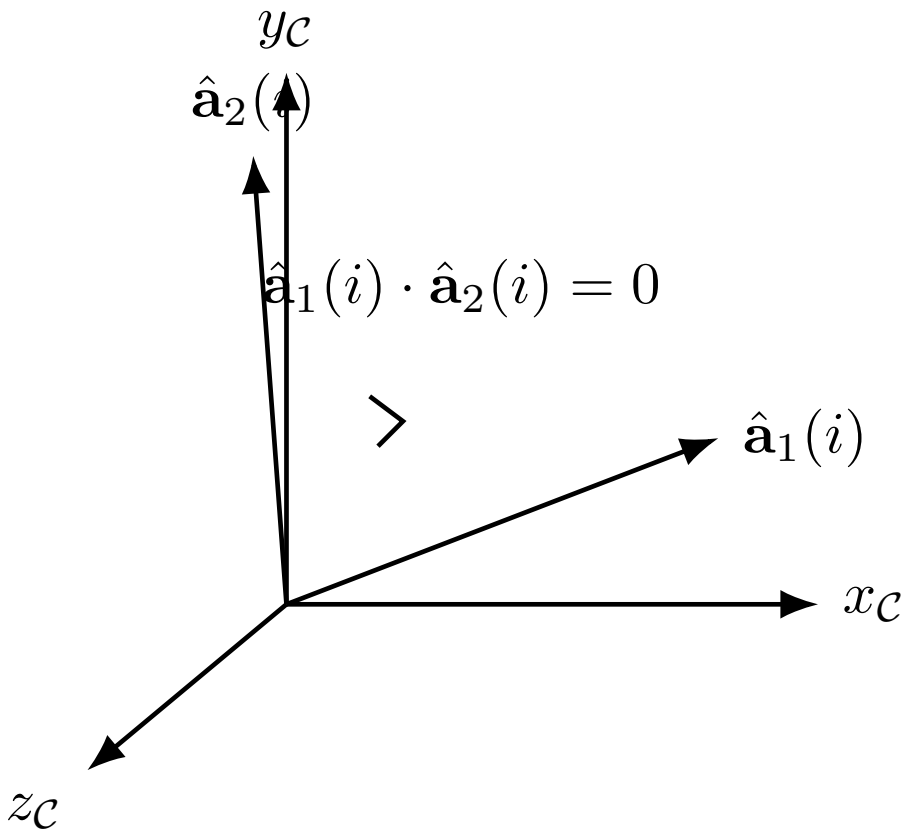

Figure 3: Schematic depiction of orthogonal afocal axes in the camera frame for a fixed tumbler state i.

6 Full Forward Model (Geometry + Radiometry)

Define the full observation operator for configuration (i, p, b) as:

$$\mathbf{x} = \Pi_{i,p,b}(\hat{\mathbf{u}}) \triangleq \pi_b\big(\Phi_{p,b}\big({}^{\mathcal{C}}\mathbf{R}_{\mathcal{D}}(i)\,\hat{\mathbf{u}}\big)\big)\,. \tag{14}$$

Radiometrically, let the scene radiance (or band-appropriate intensity) along direction $\hat{\mathbf{u}}$ be $L_b(\hat{\mathbf{u}})$. The measured pixel value $y_{i,p,b}(\mathbf{x})$ at $\mathbf{x}$ is:

$$y_{i,p,b}(\mathbf{x}) = g_{i,p,b}\, L_b(\hat{\mathbf{u}}) + o_{i,p,b} + \eta, \tag{15}$$

where $g_{i,p,b}$ is gain, $o_{i,p,b}$ is offset, and η is a noise term.

7 Integrated Calibration Source as an Anchor Measurement

Let the device include at least one uniform temperature calibration source. Model it as an approximately Lambertian emitter with known temperature T and emissivity ϵ. In each band b, it produces a known band radiance $L_b^{\text{cal}}(T)$ (e.g., integrated Planck radiance over the bandpass).

Let $\Omega_{i,p,b}^{\text{cal}} \subset \mathbb{S}^2$ denote the set of ray directions (in camera coordinates) that intersect the calibration source when configuration (i, p, b) is selected. Let $\mathcal{X}_{i,p,b}^{\text{cal}} \subset \mathbb{R}^2$ denote the set of pixels imaging the calibration source under that same configuration.

For any pixel $\mathbf{x} \in \mathcal{X}^{\text{cal}}_{i,p,b}$ imaging the calibration source, the ideal expected response is:

$$\mathbb{E}\left[y_{i,p,b}(\mathbf{x})\right] = g_{i,p,b}\, L^{\text{cal}}_b(T) + o_{i,p,b}. \tag{16}$$

Thus, for each configuration (i, p, b), one may estimate $(g_{i,p,b}, o_{i,p,b})$ via regression over calibration pixels:

$$\min_{g,o} \sum_{\mathbf{x}\in\mathcal{X}^{\text{cal}}_{i,p,b}} \Big(y_{i,p,b}(\mathbf{x}) - (g\, L^{\text{cal}}_b(T) + o)\Big)^2. \tag{17}$$

Diagram: Calibration Anchor Within the Configuration Graph

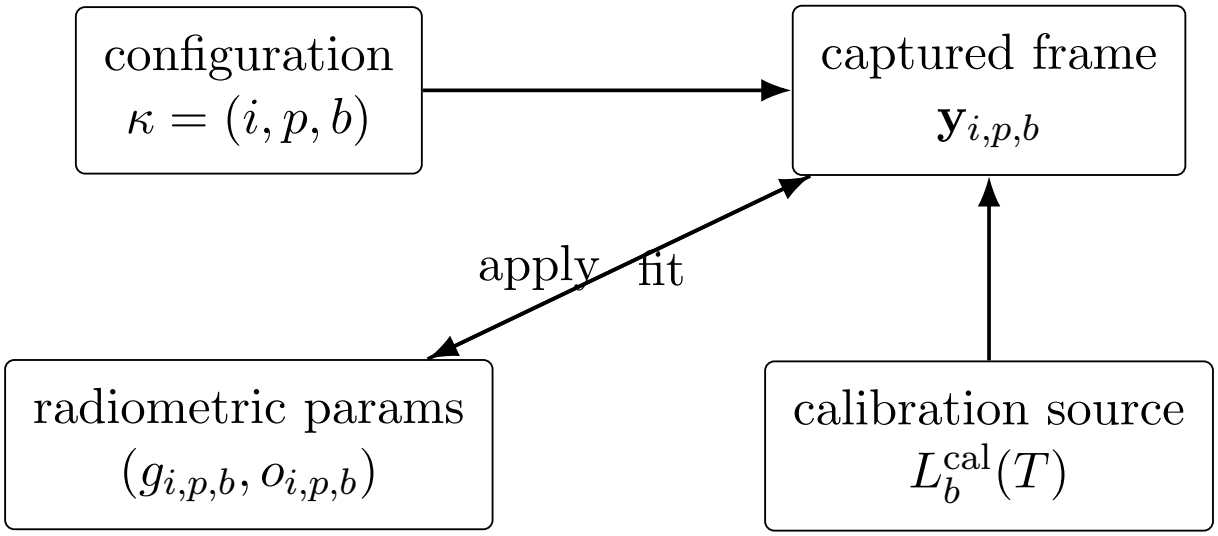

Figure 4: The uniform-temperature calibration source provides an anchor enabling configuration-indexed estimation of radiometric parameters.

8 Cross-Mode Consistency and Drift Detection

Because the calibration source is observed through multiple tumbler states, optical channels, and spectral bands, it provides an Orthospace "anchor" that enables configuration-indexed drift monitoring.

Define the residual for configuration (i, p, b):

$$r_{i,p,b}(\mathbf{x}) \triangleq y_{i,p,b}(\mathbf{x}) - \left(\hat{g}_{i,p,b}\, L^{\text{cal}}_b(T) + \hat{o}_{i,p,b}\right). \tag{18}$$

Define the mean residual and residual variance:

$$\mu_{i,p,b} = \frac{1}{|\mathcal{X}^{\text{cal}}_{i,p,b}|} \sum_{\mathbf{x}\in\mathcal{X}^{\text{cal}}_{i,p,b}} r_{i,p,b}(\mathbf{x}), \quad \sigma^2_{i,p,b} = \text{Var}_{\mathbf{x}\in\mathcal{X}^{\text{cal}}_{i,p,b}}\big[r_{i,p,b}(\mathbf{x})\big]. \tag{19}$$

9 Orthospace Fusion: Mapping Multiple FOVs into a Common Latent Field

Let $\mathcal{S}$ denote a latent scene parameterization in a common coordinate domain (e.g., a spherical environment map or a 3D scene representation). Orthospace fusion treats each configuration as a structured projection from $\mathcal{S}$ to the measured image:

$$\mathbf{y}_{i,p,b} = \mathcal{H}_{i,p,b}(\mathcal{S}) + \eta. \tag{20}$$

A generic maximum likelihood or MAP estimate of $\mathcal{S}$ may be formed by minimizing:

$$\min_{\mathcal{S}} \sum_{i,p,b} \|\mathbf{W}_{i,p,b}\,(\mathbf{y}_{i,p,b} - \mathcal{H}_{i,p,b}(\mathcal{S}))\|_2^2 + \lambda\,\mathcal{R}(\mathcal{S}), \tag{21}$$

where $\mathbf{W}_{i,p,b}$ weights measurement confidence (noise, vignetting, motion during rotation) and $\mathcal{R}$ is a regularizer.

Because the two afocal assemblies are orthogonal, $\{\mathcal{H}_{i,p,b}\}$ spans complementary subspaces of the latent scene, improving conditioning and reducing ambiguity relative to a single-axis multi-magnification approach.

10 Configuration Metadata and Deterministic Selection

Each acquired frame can be labeled by its configuration tuple:

$$\kappa \triangleq (i, p, b) \in \mathcal{I} \times \mathcal{P} \times \mathcal{B}. \tag{22}$$

11 Summary of Orthospace Contribution

The Orthospace formulation is the structured representation:

1. Discrete configuration group $\mathcal{I}$ induced by tumbler indexing;
2. Orthogonal basis axes defining complementary projection subspaces;
3. Layered band operators $\mathcal{B}$ sharing a common geometric latent space;
4. Embedded radiometric anchor via the calibration source enabling configuration-indexed normalization and drift detection;
5. Composable forward model $\Pi_{i,p,b}$ enabling cross-FOV registration and multi-band fusion without re-deriving independent camera models.

This formalism yields a unified, configuration-aware, calibration-anchored model for multi-FOV dual-band imaging through a modular, electro-mechanically selectable afocal tumbler assembly.